Werk

Jahr: 1976
Kollektion: fid.geo
Signatur: 8 Z NAT 2148:42
Digitalisiert: Niedersächsische Staats- und Universitätsbibliothek Göttingen
Werk Id: PPN1015067948_0042
PURL: http://resolver.sub.uni-goettingen.de/purl?PPN1015067948_0042

LOG Id: LOG_0080
LOG Titel: Electromagnetic scale model experiments for the coastline effect of geomagnetic variations
LOG Typ: article

Übergeordnetes Werk

Werk Id: PPN1015067948
PURL: http://resolver.sub.uni-goettingen.de/purl?PPN1015067948
OPAC: http://opac.sub.uni-goettingen.de/DB=1/PPN?PPN=1015067948

Contact

Niedersächsische Staats- und Universitätsbibliothek Göttingen
Georg-August-Universität Göttingen
Platz der Göttinger Sieben 1
37073 Göttingen
Germany
Email: gdz@sub.uni-goettingen.de

J. Geophys. 42, 507–520, 1977

Journal of Geophysics

Electromagnetic Scale Model Experiments for the Coastline Effect of Geomagnetic Variations

P. Spitta

Institut für Geophysik der Universität Göttingen,
Herzberger Landstr. 180, D-3400 Göttingen, Federal Republic of Germany

Abstract. Geomagnetic induction problems at coastlines and edges are studied on a reduced scale. Aluminium conductors are used to represent the oceans and conducting matter at greater depth within the earth. In the two-dimensional case the direction of the edges is either perpendicular or parallel relative to the inducing magnetic field (*E*- or *H*-polarization). In the three-dimensional case two edges are intersecting at right angles, forming a superposition of both polarizations. Measurements of the total magnetic field in three components are carried out over the whole area of each of the three scale models, showing the different behaviour of the models when exposed to the inducing field. In order to show the pattern and strength of the induced currents, an equivalent current system in the plane of observation is introduced. Measurements across the coast of California are interpreted by an appropriate scale model.

Key words: Scale model experiments – Geomagnetic induction – Equivalent current system

1. Introduction

The interpretation of induced magnetic fields, observed at the earth's surface above an internal conductivity distribution, is generally done by assuming an electrical conductivity model with several free parameters, which in turn are adjusted to the data either by model calculations or by scale model experiments. Both methods have to simplify the geometry of the inducing field as well as the structure of the conducting matter within the earth, in which the induced currents are flowing. Model calculations are confined more or less to two-dimensional structures [Schmucker, 1973] although progress is made in treating three-dimensional conductivity distributions [Jones, 1973; Weidelt, 1975].

These limitations are not to be found in scale model experiments, they can be readily used to study rather complex three-dimensional induction prob-

lems, if only the conductivity contrast in nature is large enough to be modelled with the existing materials. It is more difficult to produce small differences in conductivity than great ones because of the lack of appropriate materials. Dosso [1973] uses the contrast between graphite as a good and an electrolytic solution as a poor conductor, the conductivity ratio is in the order of $10^4:1$ or greater. Hermance [1968], Launay [1970], and Spitta [1973] are studying the coast effect by using the conductivity contrast between metal and air, which is much greater, and the effect tends to be overestimated [Hermance, 1968]. But at a conductivity contrast of $10^4:1$ it is anyhow unlikely for the induced currents in the metal to penetrate into the poor conductor to close the current-loops. Bearing this in mind, the deviation from reality will be small, when the poorly conducting layers on land are replaced by air in model experiments.

Maxwell's field equations are invariant against changes of scale in time and space, if for a quasi-stationary electromagnetic skin-effect problem the condition for physical similarity under change of scale

$$\frac{\omega_m}{\rho_m} d_m^2 = \frac{\omega_n}{\rho_n} d_n^2 \tag{1}$$

is satisfied. Here ω, ρ, and d denote the frequency, the resistivity, and a characteristic linear dimension, the subscript m refers to the model, the subscript n to nature. For any corresponding pair of points in model and nature Equation (1) must be valid. An example of the transformation between nature and scale model is given in Table 1 in Section 4.

2. The Experimental Arrangement

The experimental set-up has been reported elsewhere [Spitta, 1973]. Hence, only recent improvements are mentioned here. They are described in detail by Spitta [1975]. Now, the phase meter admits phase determinations in the full range from 0° to 360° instead of the former range from 0° to 180°. This allows the recording of all phase angles in respect to the reference voltage. The reference voltage is produced by the inducing current as a voltage drop on a small resistance, which replaces the transformer used before. The phase shifter is no longer necessary and therefore omitted.

The arrangement of the field generating coil, the pick-up coils for field measurements, and the scale model are shown in Figure 1. A system of right-handed rectangular coordinates x, y, and z is adopted. Its origin is the centre of the lower side of the coil, z points downwards, x is directed parallel to the axis of the coil, and y is the direction of the currents of the inducing field. H_x, H_y, and H_z are the amplitudes of the components of the magnetic field in the appropriate directions, or, with an additional subscript R or I, the in-phase or out-of-phase parts of the magnetic field, respectively.

The pick-up coils for the magnetic field components are driven 66 cm below the rectangular field-generating coil on a rigid beam by a pulley-and-belt system, allowing a continuous recording of amplitudes and phases for traverses across the model. These profiles can be shifted parallel to each other to measure

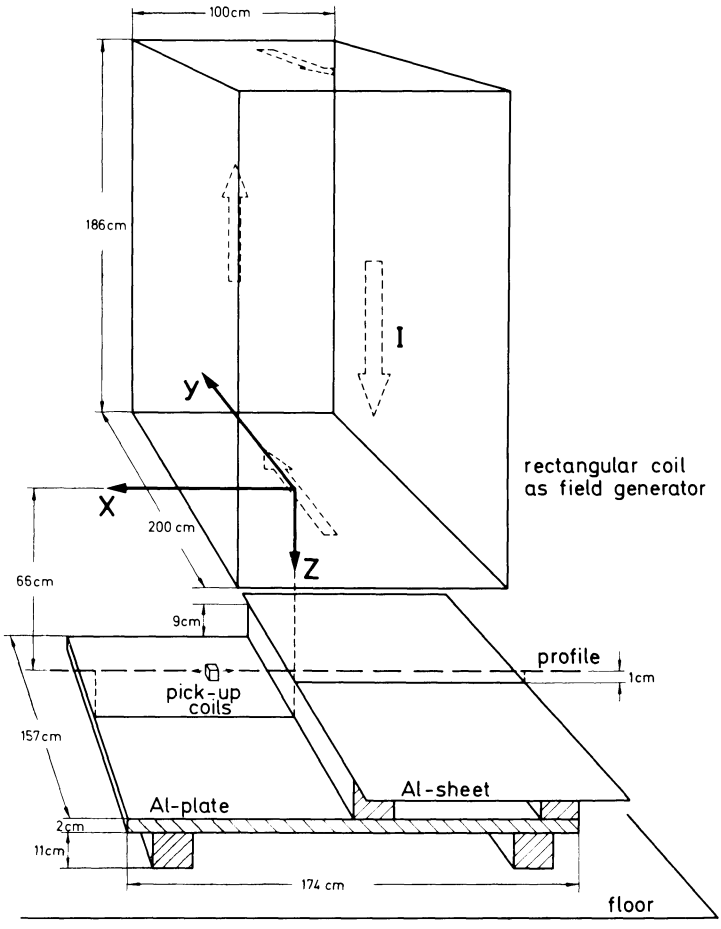

Fig. 1. Diagram of the model measurement system. The rectangular coil with 100 turns per meter of copper wire and with the axis directed in the x-direction produces the magnetic field that induces currents in the scale model below. The total magnetic field is scanned by a small pick-up coil tripel between the rectangular coil and the model. The profile in x-direction can be shifted both in y- and z-direction. For an inducing current of 1 A the magnetic field intensity in the level of the Al-sheet is of the order of 10 A/m. The model shown is that of the half-sheet anomaly in E-polarization (cf. Fig. 4)

the magnetic field at each point of the model. The aluminium plate, which represents the conducting mantle within the earth, is situated 76 cm below the field generating coil. Anomalies near the surface of the earth, e.g. the coast effect, are being modelled by thin aluminium sheets 9 cm above the aluminium plate, as shown in Figure 1.

The comparison of the measured magnetic field on the central profile ($y=0$, $z=66$ cm), measured without conductor at a frequency of 215 Hz, with the computed values of the magnetic field of the coil for free space shows a good agreement (Fig. 2). The small difference between the two curves is due to induction in the steel reinforced concrete floor. The phases of the measured

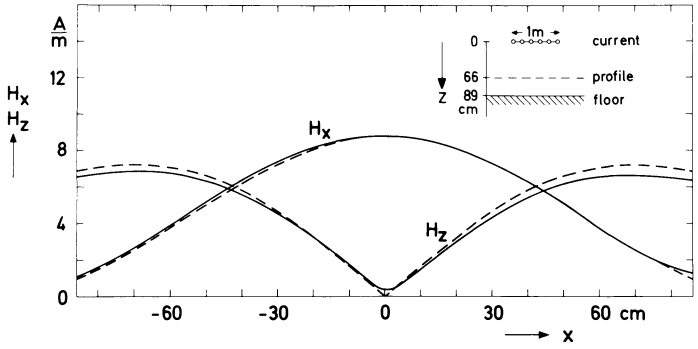

Fig. 2. Magnetic field amplitudes H_x and H_z of a 100 cm sheet current for the frequency 215 Hz, measured across a profile placed 66 cm below the current system at $y=0$ (solid lines), compared with the calculated magnetic field for free space along the same profile (dashed line). The deviation of the two curves is due to the induction in the steel-reinforced concrete of the floor

magnetic field deviate very little from 0° or 180° and therefore they are not shown.

The measured amplitudes and phases are converted in in-phase and out-of-phase parts, which are equivalent to amplitude and phases, but allow further mathematical treatment such as subtracting the inducing field to get the magnetic field of the induced currents alone. The conversion formulas are given by the following equations:

$$H_R = H \cdot \cos\phi \tag{2}$$

$$H_I = H \cdot \sin\phi, \tag{3}$$

H_R denotes the in-phase part (R=real part), H_I the out-of-phase part (I=imaginary). H is the amplitude, ϕ the phase lead of the observed field component relative to the inducing field, generated by the coil above the model.

In nature induction takes place everywhere according to the conductivity of the earth. The conductivity is not only determined by the chemical and mineralogical composition of the rocks, the porosity and the contents of salt solution, but also by the temperature. At increasing temperature the semiconducting nature of the rocks becomes evident [Keller, 1971; Schult, 1974]. It can be stated that sufficiently low resistivities around 1 Ωm exist within the earth's mantle at several hundred kilometers depth. They are covered by relatively poor conductors of at least 100 Ωm resistivity [Rikitake, 1966].

For an inducing magnetic field of external origin the measurements on the earth's surface yield an enhancement of the horizontal components and a decrease of the vertical component of the total field due to the induced currents within the earth. According to the transformation formula (1) of Section 1 this is valid also for scale models, as it is demonstrated in Figure 3. Here the x- and z-components of the magnetic field across the aluminium plate (solid line) are compared with the measured field without Al-plate (dash-dotted line). The thickness of the Al-plate (2 cm) is more than 3 times the penetration depth (0.58 cm) for 215 Hz, therefore the plate can be regarded as infinitely thick for 215 Hz or higher frequencies.

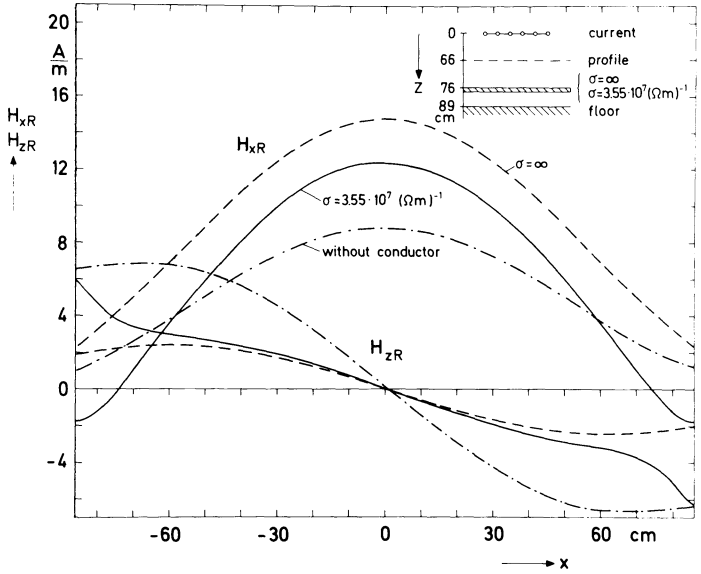

Fig. 3. In-phase parts H_{xR} and H_{zR} of the total magnetic field, measured across a profile in the x-direction 66 cm below the coil. The field is composed of the fields of the inducing sheet current and the induced currents in an Al-plate 76 cm below the current system. The plate has a conductivity of $3.55 \cdot 10^7$ $(\Omega m)^{-1}$ and a thickness of 2 cm, the frequency is 215 Hz (solid line). These curves are compared with the magnetic field across a half-space of infinite conductivity, calculated for the same profile (dashed line), and with the measured magnetic field (real parts) for the same profile without conductor below (dash-dotted line)

On the other hand comparing the measurements across the Al-plate (solid line) with the computed field above a half-space of infinite conductivity (dashed line), there is a discrepancy between the 2 curves. The magnetic field above a half-space can be computed as a superposition of the inducing field and the induced field, which is a reflection of the inducing field at the surface of the half-space. It can be shown by an approximation formula by Pollaczek [1926] that the difference in the surface fields due to infinite and finite conductivity ($\sigma = 3.55 \cdot 10^7$ $(\Omega m)^{-1}$) is less than 1%. Therefore the dashed curves in Fig. 3 represent the theoretical field for an infinitely conductive half-space as well as for an half-space with $\sigma = 3.55 \cdot 10^7$ $(\Omega m)^{-1}$. It is obvious, that the induced currents in the aluminium plate are weaker than the currents to be expected in the half-space. The current loops in the half-space are closing at infinity, whereas the currents in the plate have to form closed loops within the dimensions of the plate. The horizontal magnetic field of the return currents at the edge of the plate overcompensates the inducing field, leading there to a reversal of the horizontal magnetic field. Therefore the in-phase horizontal x-component of the magnetic field is decreased around the centre of the plate, whereas the in-phase vertical z-component is slightly increased near the edge. This effect arising from the limited dimensions of any scale model has to be kept in mind when planning a scale model experiment.

3. Experimental Results

Edge effects such as the coast effect have been treated by various authors both as scale models and model calculations. A summary and a comparison of these works is given by Dosso [1973]. The present paper investigates the response of a coast line to inducing magnetic fields perpendicular and parallel to the edge (*E*- and *H*-polarization) [Schmucker and Jankowski, 1972]. Measurements for both polarizations are plotted seperately in Figures 4 and 6. The model consists of an aluminium plate of the size of $174\,\text{cm} \times 157\,\text{cm} \times 2\,\text{cm}$, which represents the highly conducting mantle at a depth of 360 km, and an aluminium sheet, $180 \times 100\,\text{cm}^2$ in area and 0.1 cm thick, placed 9 cm above the plate. It simulates an ocean with the depth of 4 km with a sea water resistivity of $0.25\,\Omega\text{m}$. It can be regarded as a thin sheet in the sense that its thickness is small in comparison to the skin depth at the experimental frequency. With this change of length scale and resistivity the frequency of 215 Hz corresponds in nature to a period of 3.7 h, according to the transformation formula (1). No electrical contact exists between sheet and plate.

In Figure 4 the sheet has been placed at the right hand side, extending from $x=0$ to $x=-100\,\text{cm}$ and from $y=-80\,\text{cm}$ to $y=+80\,\text{cm}$, forming a half-sheet anomaly in *E*-polarization. It can be seen both in the in-phase and out-of-phase parts, that the x-component suddenly increases across the coast from "land" to "ocean" and remains enhanced above the sheet due to the induced currents in the sheet. The same currents produce a decrease of amplitude in the in-phase z-component above the sheet, whereas the out-of-phase z-component is enhanced. A strong coast effect in the z-component is to be seen immediately at the edge. Since in the y-direction no conductivity contrast is encountered, almost no anomalous behaviour in the y-component is found. A comparison of measurements across the coast of California and an appropriate scale model is given in Section 4.

In order to show the pattern and strength of the induced currents, flowing in the sheet above the aluminium plate, an equivalent sheet current distribution in the level of observation 1 cm above the thin sheet is introduced. The magnetic field of the induced currents can be found by subtracting the measured magnetic field without sheet (but including the Al-plate), as shown by solid lines in Figure 3, from the magnetic field across the whole model including the Al-sheet (Fig. 4), in in-phase and out-of-phase parts. Since the distance between the plane of observation and the sheet is small compared with the horizontal dimensions of the sheet, it is assumed that the current system derived from the magnetic field in the plane of observation is similar to the true current system on the sheet. Let $\hat{\mathbf{z}}$ be the unit vector in z-direction. Then the equivalent sheet-current density $\mathbf{j}$ connected with the magnetic field $\mathbf{H}$ at point $\mathbf{r}$ is given by

$$\mathbf{j}(\mathbf{r}) = -2\,\hat{\mathbf{z}} \times \mathbf{H}(\mathbf{r}). \tag{4}$$

In the equivalent current density plots of Figures 5, 7, and 9 direction and strength of $\mathbf{j}$ are represented at equally spaced points in a rectangular grid by direction and length of arrows.

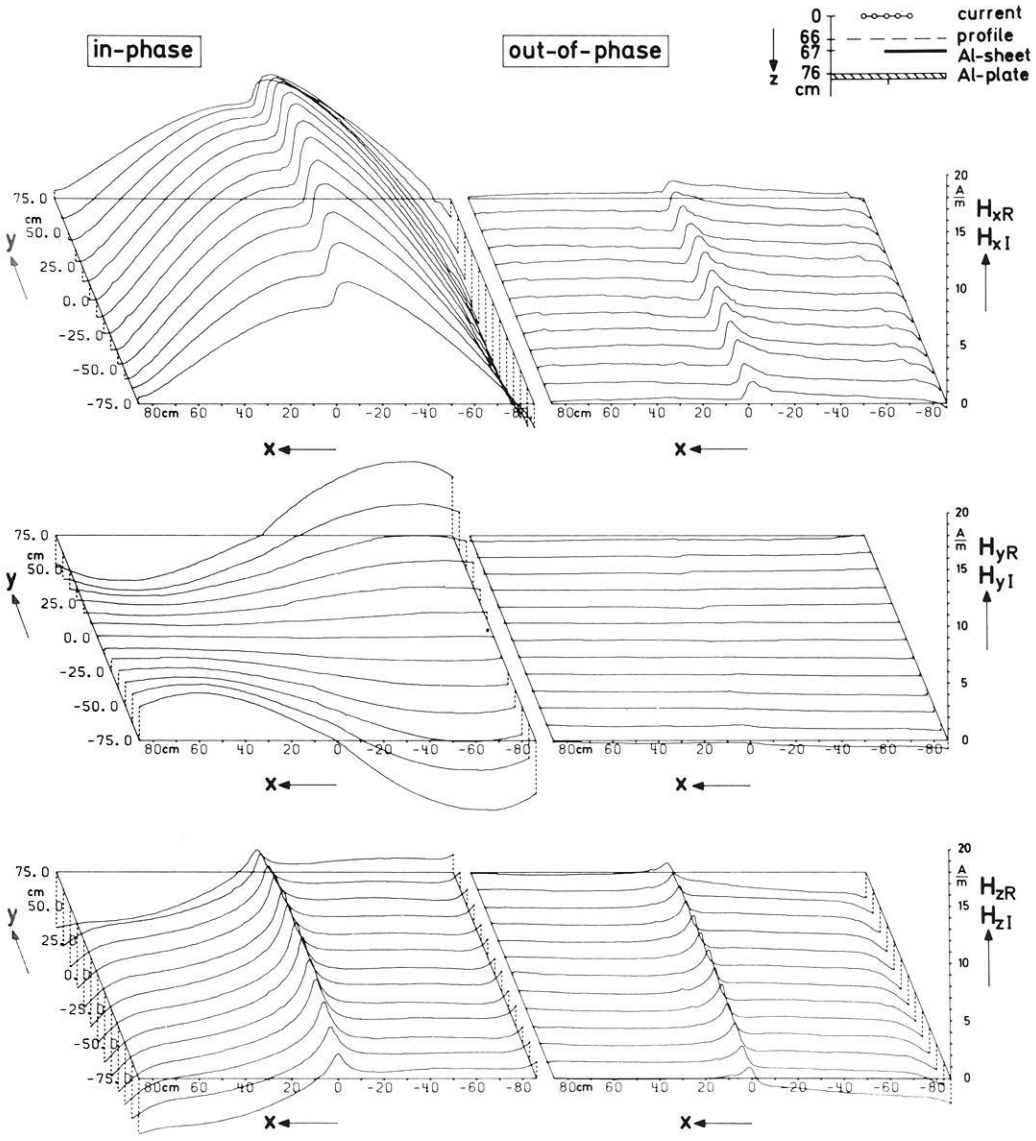

Fig. 4. Edge-effect in *E*-polarization: In-phase parts (left) and out-of-phase (right) of the magnetic field components H_x, H_y, and H_z, measured 66 cm below the coil over the whole area of the scale model, which consists of a thin Al-sheet, partly covering an Al-plate 9 cm below. The half-sheet extends from $x=0$ to $x=-100$ cm, the frequency used is 215 Hz

The equivalent currents density arrows for the aluminium sheet are shown in Figure 5. Only the in-phase parts of the induced currents are considered here. As expected, the currents in the sheet are forming an elongated eddy. The fairly small currents outside the sheet can be attributed to two effects. First, the distribution and strength of the magnetic field of the equivalent currents depends on the distance of the plane of observation from the sheet. The

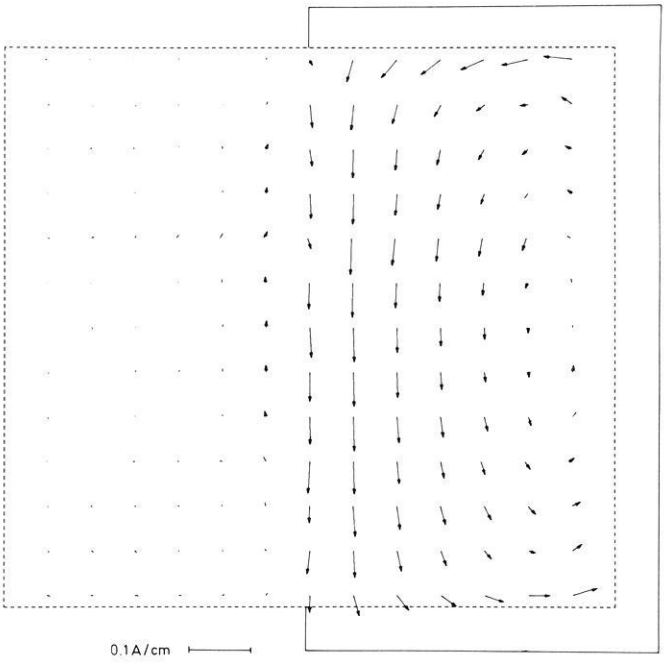

Fig. 5. Equivalent current density arrows in the half-sheet in *E*-polarization (Fig. 4), as seen from the plane of observation. The arrows which are starting at equally spaced grid points represent in direction and strength the in-phase parts of the induced surface current density vectors

lines of force of the induced currents in the sheet tend to spread into space and show in the plane of observation "equivalent currents" just in the neighbourhood of conductors. That can be seen in Figure 5 left of the edge of the sheet. Secondly, the currents in the two conducting layers of sheet and plate are influencing each other. The induced currents in the plate section beneath the Al-plate will be somewhat smaller than in the absence of the sheet. Therefore the induced field from the plate alone, which is subtracted, is too large. Consequently, small equivalent currents outside the sheet remain [Spitta, 1975].

With regard to the coast in *H*-polarization the response of the sheet is quite different. For that purpose the sheet is turned by 90° and placed at the rear side of the scale model of Figure 1. The sheet extends from $y=0$ to $y=+100\,\text{cm}$ and from $x=-80\,\text{cm}$ to $x=+80\,\text{cm}$. The edge of the sheet is parallel to the most intense x-component of the inducing field. Since the changes of the magnetic field along a profile are more prominent perpendicularly to the edge, the direction of the profiles has been changed too, as it can be seen in Figure 6. Here y is directed from right to left, parallel to the profiles, the x-direction is from the rear side to the front. The ordinate is the intensity of the magnetic field in in-phase and out-of-phase parts. The sheet is lying on the left hand side, as indicated by the model sketch in the upper right corner. Since no change in conductivity is encountered, the amplitude in the

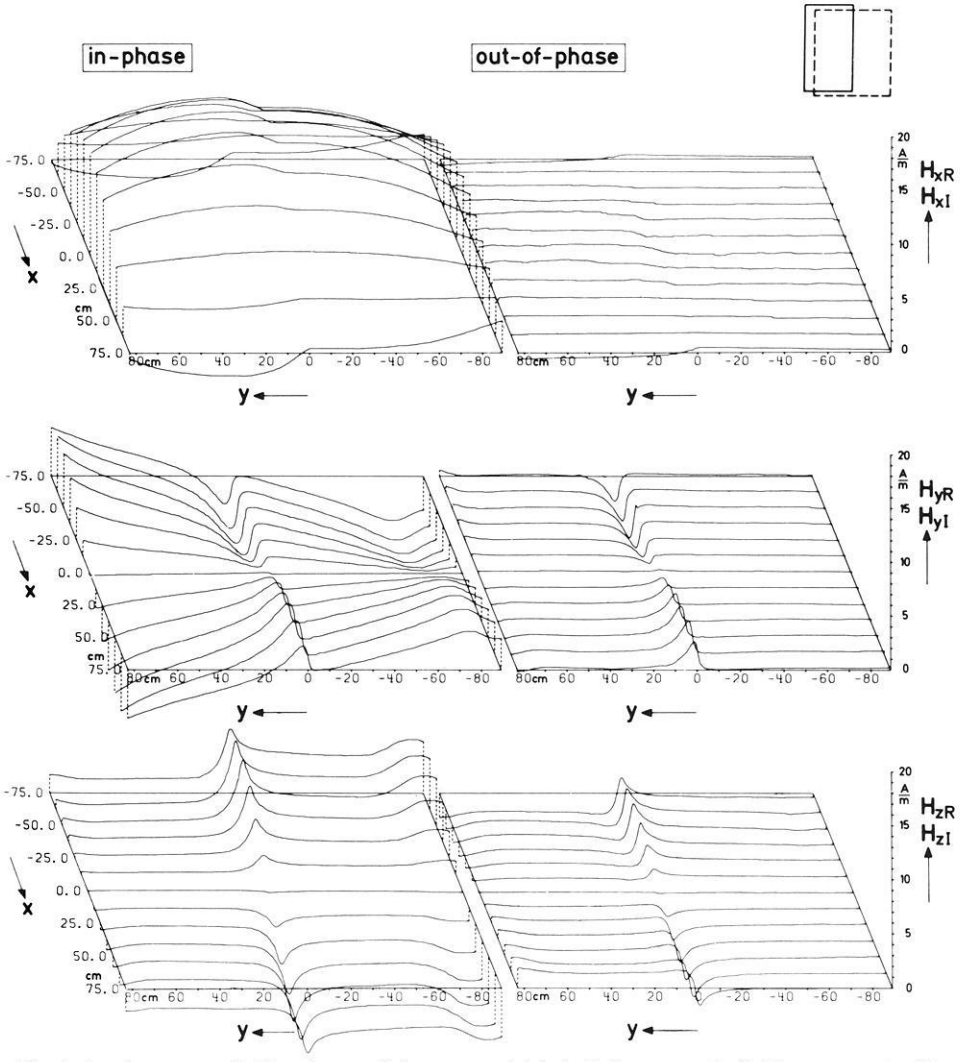

Fig. 6. In-phase parts (left) and out-of-phase parts (right) of the magnetic field components H_x, H_y, and H_z for the edge effect in H-polarization. The Al-sheet, which is partly covering the Al-plate, extends from $y=0$ to $y=+100$ cm

x-component is not affected by the edge (disregarding the extreme profiles at $y=\pm 75$ cm). But the currents, induced by the x-component, are flowing in the y-direction and are forced by the edge to change their direction: they have to flow in the positive or negative x-direction. Their magnetic fields contribute to the magnetic field in y-direction, but opposite in sign to the inducing field. So the coast effect is shown by the y-component here, similar in strength as the x-component in E-polarization. In the z-component only the different geometry of the inducing field is to be seen as a new effect. The equivalent current density arrows (real parts) for the half-sheet in H-polarization are shown in Figure 7.

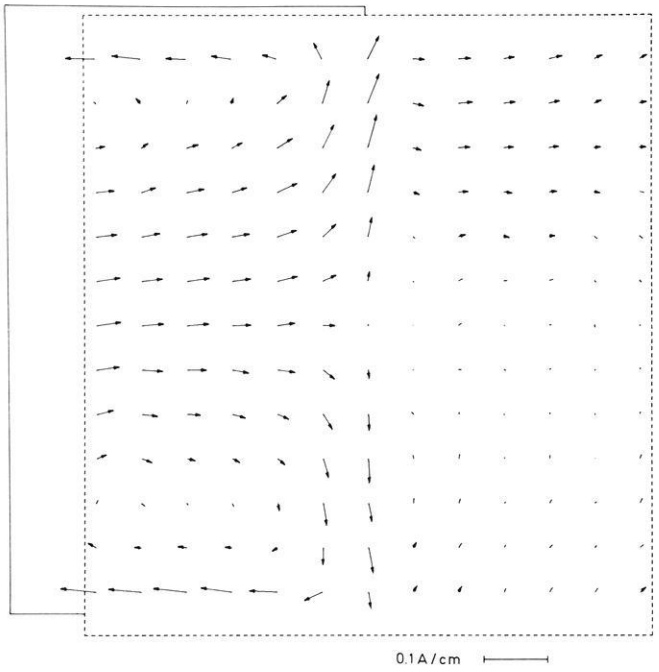

Fig. 7. Equivalent current system in the half-sheet in *H*-polarization (Fig. 6), representing the density of the in-phase parts of the induced currents in the sheet

The half-sheet anomalies in *E*- or *H*-polarization can be treated as 2-dimensional structures, they are still tractable by model calculations [Schmucker, 1971]. In spite of the progress in three-dimensional model calculations more complicated coast lines, as the coastline of southwestern Australia [Everett and Hyndman, 1967], require scale model experiments for the interpretation of the observation in nature. Wide oceans with a depth of 3–4 km exist along the southern and western coast of Australia, which are intersecting approximately at right angles. This configuration of land and sea can be modelled by 2 aluminium sheets, representing the oceans, placed one upon another, forming an angle of 90°, and covering three quadrants of the aluminium plate. They are not in electrical contact with each other, the aluminium plate being placed 9 cm below the sheet. Now the effect of two edges is expected, one along $x=0$ for the sheet in "*E*-polarization", and the other along $y=0$ for the sheet in "*H*-polarization". The edge effects will be less pronounced at points where the sheets cover each other.

This is evident when comparing single profiles of the half-sheet anomaly in *E*-polarization and the just mentioned corner anomaly. Figure 8 shows three profiles across the half-sheet as solid lines and three profiles across the corner anomaly as dashed lines. Hardly any difference is to be seen in the x-component at the profiles at $y=0$ and $y=-50$ cm, in the y-component at $y=-50$ cm and $y=+50$ cm, and in the z-component at $y=-50$ cm due to the almost same geometry. The effect of the induced currents in the second sheet which

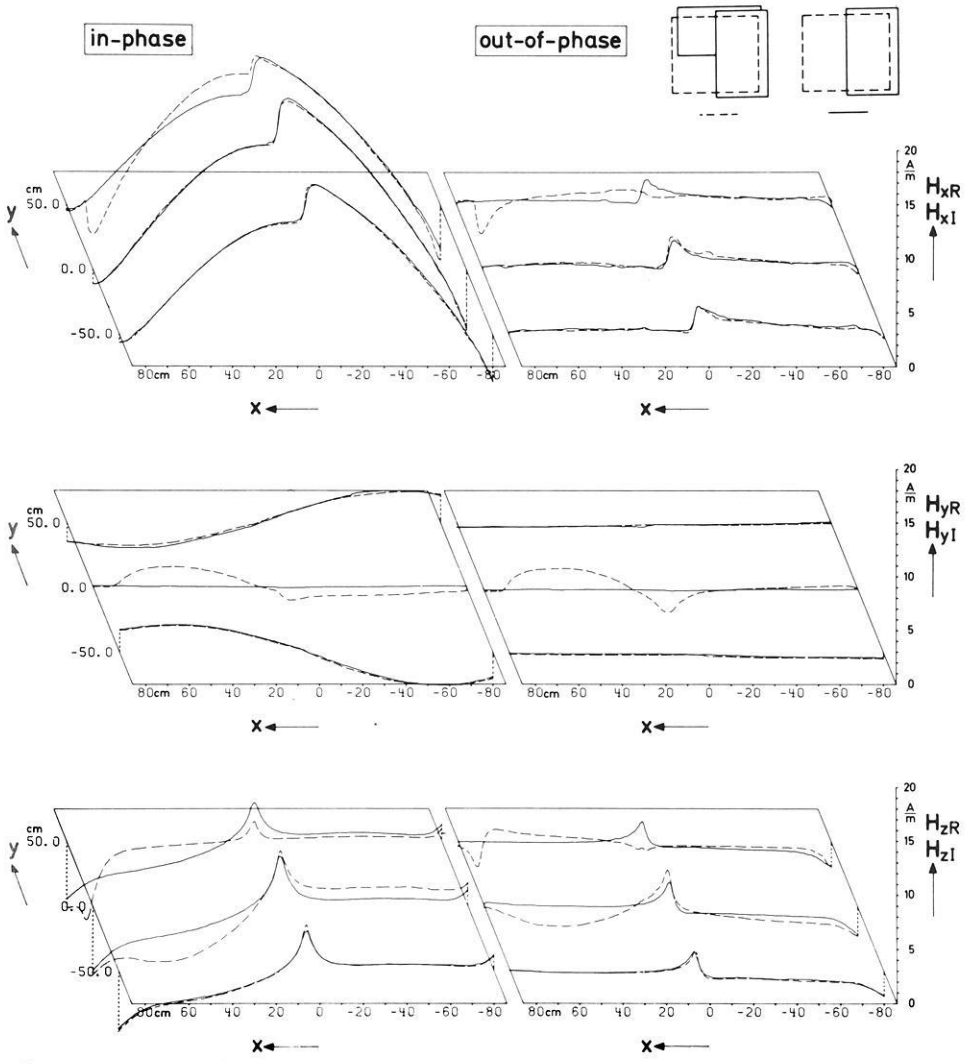

Fig. 8. Comparison of single profiles of the half-sheet anomaly in E-polarization (solid lines) and the corner anomaly (dashed lines). The corner anomaly consists of two Al-sheets forming a right angle, covering three-quarters of the Al-plate 9 cm below. Drawn are on the left the in-phase parts, on the right the out-of-phase parts of the magnetic field components H_x, H_y, and H_z

is in "H-polarization" is seen in the difference between the two curves in the x- and z-component at $y=+50$ cm. At $y=0$ the edge effect is clearly demonstrated in the y- and z-component. Here H_{yR} and H_{yI} increase in amplitude from almost zero for a single half-sheet (solid line) to a substantial edge anomaly on the left hand side of the profile (dashed line). The z-component has a pronounced peak at the corner point ($x=0$, $y=0$) and preserves a remarkable amplitude along the edge of the second half-sheet parallel to x.

The equivalent current density arrows (real parts) for this scale model are shown in Figure 9. It makes a difference whether the half-sheet with the edge

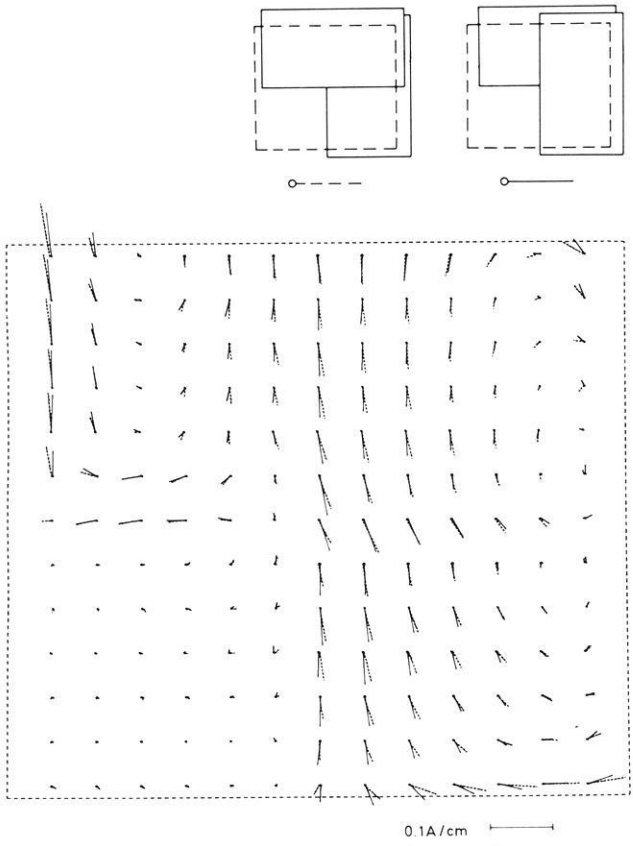

Fig. 9. Equivalent current system in the half-sheets of the corner anomaly, presented by two different arrangements of the sheets. The arrows are representing the density of the in-phase parts of the induced currents in the sheet

in y-direction is placed on top or below the second half-sheet with the edge in x-direction. The currents of both arrangements are plotted in the same picture "y-sheet on top" with solid lines, "y-sheet below" with dashed lines. The currents are forming two eddies, separated by the edge at $x=0$ in the case the y-sheet is on top, whereas the line of separation is shifted more to the left in the case the y-sheet is below. The difference between the two arrangements turns out to be mostly a deviation in direction of the currents with only slight differences in amplitude.

4. Application of Scale Models

In this last section an application of scale models is given by interpreting actual measurements across a coast. Since the depth of the sea water on the continental shelf is small (about 100 m) compared with the deep ocean (about 3 km), the shelf can be regarded as belonging to the land. Referring to Table 1 where modelling data are compared with data from nature, the depth of water on the shelf would be represented in the model by a very thin foil (0.03 mm),

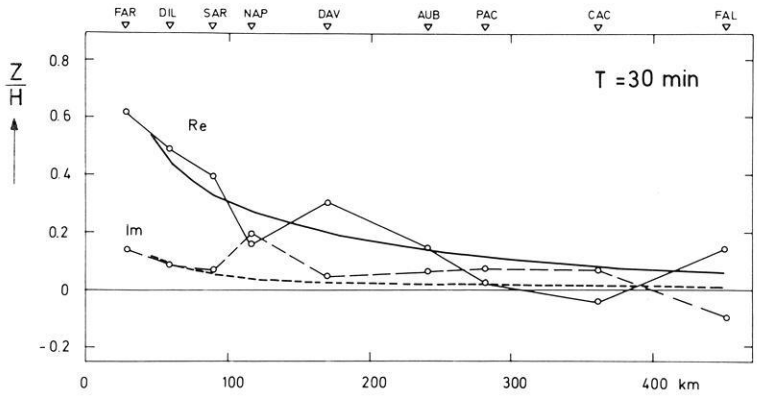

Fig. 10. Comparison between measurements (small circles) and transformed scale model results for the ratio of the anomalous Z to the normal H across the coast of California. The scale model results refer to the plane of the sheet, in-phase and out-of-phase parts are drawn by solid and dashed lines, respectively. The simulated depth of the ocean is 3 km, the simulated depth of the high mantle conductivity is 270 km

Table 1. Transformation between scale model and nature by using the transformation formula (1)

Variables	Scale model	Nature
Thickness of the surface layer d	1 mm aluminium sheet	3 km ocean
Depth of the deep conductor	9 cm (aluminium plate)	270 km (conductosphere)
Resistivity ρ of the surface layer	$4.5 \cdot 10^{-8}\,\Omega$m	0.25 Ωm seawater
Frequency $\omega/2\pi$	1 kHz	$6.17 \cdot 10^{-4}$ Hz $\triangleq$ 27 min bay disturbance

that is unlikely to be seen magnetically. Therefore the "coastline" has to be placed on the continental margin, all of the measurements in nature are performed on the "land" side, the origin of the distance scale of Figure 10 is at this edge.

Figure 10 shows the ratio Z/H along a profile at the coast of California, beginning 30 km east of the edge of the continent on Farallon Island and ending near Fallon in Nevada [Schmucker, 1970]. Here H denotes the normal horizontal component perpendicular to the edge, Z the anomalous vertical component. Shown are in-phase (Re) and out-of-phase (Im) parts for a period of 30 min. The measured values are marked with small circles. For the scale model the ocean is replaced by an aluminium sheet, the conductivity of the mantle is represented by the aluminium plate, the continent by air. The geometry is quite similar to the half-sheet anomaly in E-polarization. The increase of conductivity ρ and reduction of the size d, following the transformation formula (1), is listed in Table 1. The measured values of the in-phase parts (solid line) and the out-of-phase parts (dashed line) of the scale model agree fairly well with the curves of Schmucker.

The magnetic field of the scale model has been obtained in the same level of the surface of the ocean. Hence, a small horizontal distance from the edge

had to be kept due to the size of the pick-up coils. Otherwise, by guiding the pick-up coils across the sheet at a small height of 1 cm – this corresponds to a height of 30 km above the earth's surface in nature – the curves at this altitude would be smoothed and reduced in amplitude in relation to the surface fields. Therefore it is difficult to compare then with measurements taken at the earth's surface.

Acknowledgements. I am grateful to Prof. Dr. M. Siebert for providing the basis to carry out the experiments within the scope of my thesis. I am also indebted to Prof. Dr. U. Schmucker and Dr. P. Weidelt for their helpful comments and interest in this work. Moreover, I wish to acknowledge the financial support by the Deutsche Forschungsgemeinschaft, Bad Godesberg. The numerical calculations and part of the drawings have been performed at the UNIVAC 1108 of the Gesellschaft für wissenschaftliche Datenverarbeitung in Göttingen.

References

Dosso, H.W.: A review of analogue model studies of the coast effect. Phys. Earth Planet. Interiors **7**, 294–302, 1973

Everett, J.E., Hyndman, R.D.: Geomagnetic variations and electrical conductivity structure in south-western Australia. Phys. Earth Planet. Interiors **1**, 24–34, 1967

Hermance, J.F.: Model studies of the coast effect on geomagnetic variations. Can. J. Earth Sci. **5**, 515–522, 1968

Jones, F.W.: Induction in laterally non-uniform conductors: Theory and numerical models. Phys. Earth Planet. Interiors, **7**, 282–293, 1973

Keller, G.V.: Electrical studies of the crust and upper mantle. In: The structure and physical properties of the earth's crust, J.G. Heacock, ed. Geophysical Monograph Ser. No. **14**, 107–125. American Geophysical Union, Washington D.C., 1971

Launay, L.: Modèle reduits magnéto-telluriques: principe et premiers résultats. Ann. Géophys. **26**, 805–810, 1970

Pollaczek, F.: Über das Feld einer unendlich langen wechselstromdurchflossenen Einfachleitung. Elektr. Nachrichtentechn. **3**, 339–359, 1926

Rikitake, T.: Electromagnetism and the earth's interior. Amsterdam: Elsevier 1966

Schmucker, U.: Anomalies of geomagnetic variations in the soutwestern United States. Bull. Scripps Inst. Ocean. Univ. Calif. **13**, 1970

Schmucker, U.: Neue Rechenmethoden zur Tiefensondierung. In: Protokoll „Erdmagnetische Tiefensondierung" Rothenberge/Westf., 14.–16.9.1971, P. Weidelt, ed., pp. 1–39. Institut für Geophysik, Göttingen, 1971

Schmucker, U.: Regional induction studies: A review of methods and results. Phys. Earth Planet. Interiors, **7**, 365–378, 1973

Schmucker, U., Jankowski, J.: Geomagnetic induction studies and the electrical state of the upper mantle. In: The upper mantle, A.R. Ritsema, ed. Tectonophysics, **13**, (1–4), 233–256, 1972

Schult, A.: The electrical conductivity of minerals and the temperature distribution in the upper mantle. In: Approaches to Taphrogenesis, J.H. Illies and K. Fuchs, eds., pp. 376–378. Stuttgart: Schweizerbarth 1974

Spitta, P.: Scale model experiments with solid conductors. Phys. Earth Planet. Interiors **7**, 445–449. 1973

Spitta, P.: Modellversuche zur elektromagnetischen Induktion in räumlichen metallischen Leitern mit Anwendungen auf die erdmagnetische Tiefensondierung. Diss. Math.-Nat. Fak. Göttingen. 1975

Weidelt, P.: Electromagnetic induction in three-dimensional structures. J. Geophys., **41**, 85–109. 1975

Received October 10, 1976; Revised Version December 15, 1976